



Competition studies on the activation of the C–H bond of diazines by the unsaturated triangular cluster anion $[\text{Re}_3(\mu\text{-H})_4(\text{CO})_{10}]^-$

Tiziana Beringhelli^a, Giuseppe D'Alfonso^{a,*}, Daniela Maggioni^a,
Monica Panigati^a, Pierluigi Mercandelli^{b,1}, Angelo Sironi^b

^a Dipartimento di Chimica Inorganica, Metallorganica e Analitica and CNR-ISTM, Via Venezian 21, 20133 Milan, Italy

^b Dipartimento di Chimica Strutturale e Stereochimica Inorganica and CNR-ISTM, Via Venezian 21, 20133 Milan, Italy

Received 11 November 2002; received in revised form 17 January 2003; accepted 18 January 2003

Dedicated to Professor Renato Ugo on the occasion of his 65th birthday

Abstract

The reactions of the unsaturated cluster anion $[\text{Re}_3(\mu\text{-H})_4(\text{CO})_{10}]^-$ (**1**) with 1,2-, 1,3- and 1,4-diazines (used as solvents) have been investigated. The reaction with 1,2-diazine at room temperature gives quantitatively the anion $[\text{Re}_3(\mu\text{-H})_2(\mu\text{-}\eta^2\text{-N}_2\text{C}_4\text{H}_4)(\text{CO})_{10}]^-$ (**3**), containing a diazine bridging through the two N atoms, characterised by single crystal X-ray analysis. The orthometallated isomer $[\text{Re}_3(\mu\text{-H})_3(\mu\text{-}\eta^2\text{-N}_2\text{C}_4\text{H}_3)(\text{CO})_{10}]^-$ (**4**) was obtained by refluxing **3** in toluene. The reaction of $[\text{NET}_4]\mathbf{1}$ in molten 1,4-diazine (60 °C) affords the anion $[\text{Re}_3(\mu\text{-H})_3(\mu\text{-}\eta^2\text{-N}_2\text{C}_4\text{H}_3)(\text{CO})_{10}]^-$ (**5**), containing orthometallated pyrazine. The slow reaction of $[\text{NET}_4]\mathbf{1}$ with 1,3-diazine at room temperature gives two orthometallated isomers **6**, corresponding to the metallation of carbon C2 (**6a**) and C6 (**6b**), respectively (**6b/6a** ratio ca. 1.2). Differently from what previously found for the analogous cluster anion containing orthometallated pyridine, the metallation reaction of diazines showed little reversibility, and poor conversion of **5** and **6** to the starting anion **1** was observed after several days under 100 atm of H₂. Competition experiments, performed by dissolving $[\text{NET}_4]\mathbf{1}$ in equimolar mixtures of pyridine/pyrazine or pyridine/pyrimidine, showed that the anion with metallated pyridine was the kinetically preferred product and that at longer times it slowly converted to the derivatives with metallated diazines (**5** or **6**).

© 2003 Elsevier Science B.V. All rights reserved.

Keywords: C–H bond activation; Orthometallation; Diazines; Carbonyl clusters; Rhenium

1. Introduction

The study of the reactivity of the six-member aromatic nitrogen heterocycles (azines) with transition metal clusters is an active area of research, due to

the possibility of understanding and then optimising the catalytic hydrodenitration processes [1–4]. It is known in fact that stable organometallic compounds can provide good models of the reactive intermediates in both homogeneous and heterogeneous catalytic processes. A particular interest is devoted to systems able to activate C–H bonds of organic ligands co-ordinated on metal clusters and several examples of these complexes have been described [5–18].²

* Corresponding author. Tel.: +39-02-50314351;

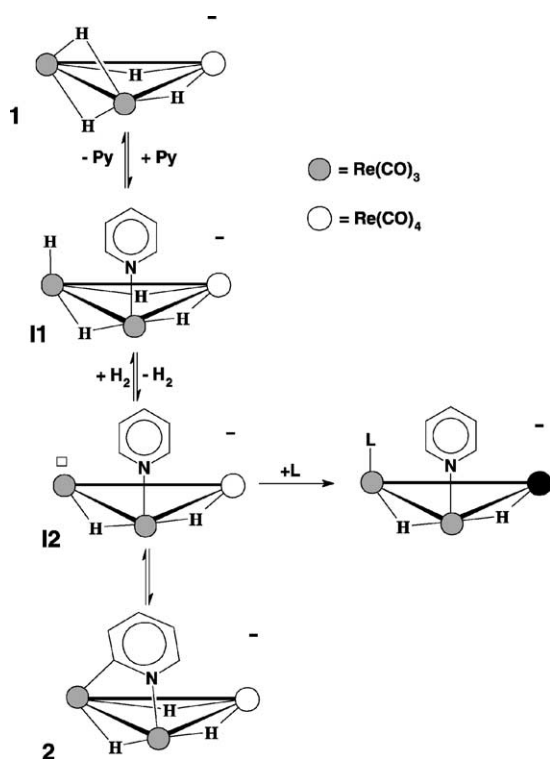
fax: +39-02-50314405.

E-mail addresses: dalf@csmtbo.mi.cnr.it (G. D'Alfonso), pierluigi.mercandelli@unimi.it (P. Mercandelli).

¹ Co-corresponding author. Tel.: +39-02-50314447;

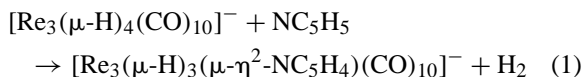
fax: +39-02-50314454.

² For studies concerning the activation of C–H bonds of nitrogen heterocycles by trisrhenium and triruthenium clusters see [13–16].

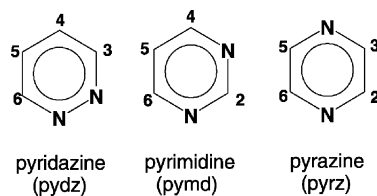


Scheme 1.

In a previous paper [19] some of us reported that the unsaturated anion $[\text{Re}_3(\mu\text{-H})_4(\text{CO})_{10}]^-$ (**1**, 46 valence electrons (v.e.s)) reacts with pyridine (Eq. (1)) at room temperature giving the anion $[\text{Re}_3(\mu\text{-H})_3(\mu\text{-}\eta^2\text{-NC}_5\text{H}_4)(\text{CO})_{10}]^-$ (**2**) containing an orthometallated pyridine molecule bridging a cluster edge.



A multi-step mechanism was proposed (see Scheme 1) in which, at first, pyridine addition on **1** gives the saturated (48 v.e.s) intermediate **11**. Fast H_2 reductive elimination affords the coordinatively and electronically unsaturated intermediate **12**, which is able to activate the $\text{C}_\alpha\text{-H}$ bond of the pyridine ligand, giving the anion **2**. Studies on using partially deuterated isotopomers [20] demonstrated the reversibility of the metallation reaction. Then in the presence of L ligands like CO, the competition between C–H



Scheme 2.

oxidative addition and CO coordination on **12** was observed, leading to a mixture of the anion **2** and of $[\text{Re}_3(\mu\text{-H})_2(\text{CO})_{11}(\text{NC}_5\text{H}_4)]^-$.

In this work we have studied the reaction of **1** with other nitrogen heterocycles, i.e. the three diazines shown in Scheme 2, with the aim of investigating new competition pathways of the intermediate **12** between: (i) C–H oxidative addition and *intramolecular* (in the case of pyridazine) or *intermolecular* (in the case of pyrazine and pyrimidine) nitrogen coordination; (ii) oxidative addition of two different *ortho* C–H bonds in the case of pyrimidine. Moreover, the competition between activation of pyridine and pyrimidine (or pyrazine) has been investigated.

2. Experimental

All reactions were performed under N_2 using the Schlenk technique in solvents deoxygenated and dried by standard methods [21]. Pyridine, pyrimidine and pyridazine were purchased from Aldrich[®] and were distilled over KOH just before the reaction, whilst pyrazine (Aldrich[®]) was used as received. $[\text{NEt}_4][\text{Re}_3(\mu\text{-H})_4(\text{CO})_{10}]$ was prepared from $[\text{NEt}_4][\text{Re}_3(\mu\text{-H})_3(\text{CO})_9]$ [22,23]. IR: Bruker Vector 22 FT, ^1H NMR: Bruker AC200 and DRX300 spectrometers.

2.1. Synthesis of $[\text{NEt}_4][\text{Re}_3(\mu\text{-H})_2(\mu\text{-}\eta^2\text{-N}_2\text{C}_4\text{H}_4)(\text{CO})_{10}]$ ($[\text{NEt}_4]\mathbf{3}$)

A sample of $[\text{NEt}_4]\mathbf{1}$ (47.5 mg, 0.049 mmol) was dissolved at room temperature in freshly distilled pyridazine (2.1 ml, 29.3 mmol). After 3 h addition of deoxygenated water (40 ml) afforded a green precipitate which was separated, washed with water, dried under vacuum and crystallised with $\text{CH}_2\text{Cl}_2/\text{Et}_2\text{O}$ (33 mg,

Table 1
IR and ^1H NMR data for the complexes described in this work

	$\nu(\text{CO})^a$ (cm^{-1})	Chemical shift δ (ppm)							
		H2	H3	H4	H5	H6	H _a ^b	H _b ^b	H _c ^b
2	2095w, 2016m, 1996vs, 1940m, 1900m,br	8.15	6.50	6.94	7.50		−12.48	−13.48	−15.15
3	2033w, 2002vs, 1957m, 1933vs, 1909s		8.67	7.07	7.07	8.67	−9.64	−12.89	
4	2093w, 2019m, 1998vs, 1945w, 1915m,br ^c			7.61 d	6.77 t	8.24 dd	−12.54	−13.29	−15.24
5	2094w, 2020m, 1997vs, 1942w, 1912m,br		8.33 d ^d		7.66 d ^d	8.05 dd ^d	−12.70	−13.56	−15.30
6a	2094w, 2019m, 1998vs, 1942w, 1910m,br			8.27 dd ^e	6.62 t ^e	8.20 dd ^e	−12.63	−13.67	−15.17
6b	2094w, 2019m, 1998vs, 1942w, 1910m,br	8.49 d ^f		7.65 d ^f	7.36 dd ^f		−12.75	−13.62	−15.34
7a ^g				7.77 dd	6.01 t	7.74 dd	−9.84	−11.28	−12.38
7b ^g		8.12		7.19	6.91		−9.77	−11.48	−12.49

^a Measured in CH_2Cl_2 at room temperature.

^b H_a indicates the hydride bridging the Re–Re edge bridged by the metallated diazine, H_b the hydride bridging the lateral edge bound to the Re atom bearing the N atom, and H_c the hydride bridging the third lateral edge.

^c Measured in toluene.

^d $J_{3,6} = 1.5$ Hz, $J_{5,6} = 3.2$ Hz from computer simulation for a AMX spin system.

^e $J_{4,5} = 5.7$ Hz, $J_{4,6} = 2.5$ Hz, $J_{5,6} = 5.1$ Hz from computer simulation for a ABX spin system.

^f $J_{2,5} = 1.2$ Hz, $J_{4,5} = 5.2$ Hz from computer simulation for a AMX spin system.

^g δ values of the protons of the terminally coordinated pyrimidine: 6.97, 8.70, 8.95 and 9.21 ppm in both the species.

0.032 mmol, isolated yields 52.8%). Slow diffusion of Et_2O into a concentrated CH_2Cl_2 solution of **3** provided crystals suitable for X-ray analysis. Spectroscopic data: see Table 1.

2.2. Reaction of $[\text{NEt}_4]\mathbf{3}$ in toluene under reflux

A sample of $[\text{NEt}_4]\mathbf{3}$ (ca. 5 mg, 4.6 μmol), suspended in freshly distilled toluene (2 ml), was refluxed for 2 h, affording an orange solution. ^1H NMR analysis showed some unreacted **3**, the novel derivative **4** and an unattributed resonance at δ −12.64 (relative integrated hydridic intensities 1:6.6:1.8). Attempts to complete the conversion of **3** into **4** with longer refluxing times (up to 6 h) led to a brown oily residue, insoluble in any common organic solvent.

2.3. Reaction of $[\text{NEt}_4]\mathbf{1}$ in molten pyrazine

A mixture of $[\text{NEt}_4]\mathbf{1}$ (10.3 mg, 10.6 μmol) and pyrazine (64.6 mg, 0.806 mmol) was heated at 60 °C for 1.5 h, then was cooled to room temperature and treated with H_2O , giving an orange oil, that was dissolved in CH_2Cl_2 . Addition of *n*-hexane gave an orange–yellow precipitate, constituted only by

$[\text{NEt}_4]\mathbf{5}$ on the bases of the ^1H NMR analysis (4.7 mg, 4.5 μmol , isolated yields 42.4%). The spectroscopic data are reported in Table 1.

2.4. Reaction of $[\text{NEt}_4]\mathbf{1}$ in pyrimidine

A sample of $[\text{NEt}_4]\mathbf{1}$ (11.7 mg, 12.0 μmol) was dissolved at room temperature in freshly distilled pyrimidine (ca. 0.5 ml, 6.3 mmol) into an NMR tube. ^1H NMR spectra were acquired until the completion of the reaction (ca. 90 h). Addition of H_2O afforded a cream precipitate of $[\text{NEt}_4]\mathbf{6}$ which was filtered and crystallised from $\text{CH}_2\text{Cl}_2/n$ -hexane (6.0 mg, 5.6 μmol , isolated yields 47%). Spectroscopic data are reported in Table 1.

2.5. Reaction of $[\text{NEt}_4]\mathbf{1}$ in pyrimidine at 85 °C

A sample of $[\text{NEt}_4]\mathbf{1}$ (10.4 mg, 10.7 μmol) in pyrimidine (0.7 ml) was heated at 85 °C for 2 h and then evaporated to dryness. The residue was dissolved in CH_2Cl_2 ; addition of Et_2O afforded an oily precipitate, that was dissolved in CD_2Cl_2 . ^1H NMR showed a number of hydridic signals, the most intense being those of **7a** and **7b** (ca. 35% of the overall integrated hydridic intensity); **6a** and **6b** were ca. 5 and 10%,

respectively, the other many weak resonances being unattributed.

2.6. Competitions between pyridine and pyrazine and between pyridine and pyrimidine

A sample of [NEt₄]**1** (8.4 mg, 8.6 μmol) was dissolved in a mixture of pyridine (280 μl, 3.45 mmol), pyrimidine (272 μl, 3.45 mmol) and acetone-*d*₆ (50 μl) directly into a NMR tube. Another sample of [NEt₄]**1** (8.9 mg, 9.1 μmol) was dissolved in a mixture of pyridine (290 μl, 3.66 mmol) and acetone-*d*₆ (50 μl) containing pyrazine (292.2 mg, 3.66 mmol). The progress of both reactions at room temperature was monitored by ¹H NMR for about 2 weeks.

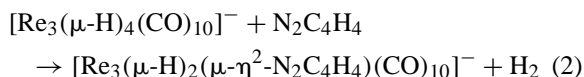
2.7. X-ray diffraction structural analysis

Crystal data for [NEt₄]**3**: C₂₂H₂₆N₃O₁₀Re₃, *M_r* = 1051.06, monoclinic, space group *P*2₁/*c* (No. 14), *a* = 8.278(1), *b* = 32.136(7), *c* = 11.868(2) Å, β = 106.34(1)°, *V* = 3029.6(9) Å³, *Z* = 4, *T* = 295(2) K, graphite-monochromated Mo Kα radiation (λ = 0.71073 Å), ρ_{calcd} = 2.304 g cm⁻³, *F*(000) = 1936, green crystal 0.20 mm × 0.12 mm × 0.12 mm, μ(Mo Kα) = 12.008 mm⁻¹, absorption correction with ψ scans of three suitable reflections [24], minimum/maximum transmission factors 0.196/0.327, Enraf-Nonius CAD-4 diffractometer, ω scans, maximum time per reflection 70 s, scan range (1.00 + 0.35 tan θ)°, 3.1 ≤ θ ≤ 24.9°, index ranges *h* = -9 → 9, *k* = 0 → 38, *l* = 0 → 14, 5278 reflections of which 2703 with *I* > 2σ(*I*), intensity decay 23%, solution by direct methods (SIR97 [25]) and subsequent Fourier synthesis, Anisotropic full-matrix least-squares on *F*² using reflections with *I* > 2σ(*I*) (SHELX97 [26]), hydrogen atoms placed in idealised position [27], data/parameters 2703/344, *S*(*F*²) = 1.078, *R*(*F*) = 0.0386, *wR*(*F*²) = 0.0652, weighting scheme *w* = 1/[σ²(*F*_o²) + (0.025*P*)² + 15*P*], where *P* = (*F*_o² + 2*F*_c²)/3, maximum/minimum residual electron density 1.060/-0.939 Å⁻³. CCDC 196631 contains the supplementary crystallographic data for this paper. These data can be obtained free of charge via <http://www.ccdc.cam.ac.uk/conts/retrieving.html> (or from the CCDC, 12 Union Road, Cambridge CB2 1EZ, UK; fax: +44-1223-336033; e-mail: deposit@ccdc.cam.ac.uk).

3. Results and discussion

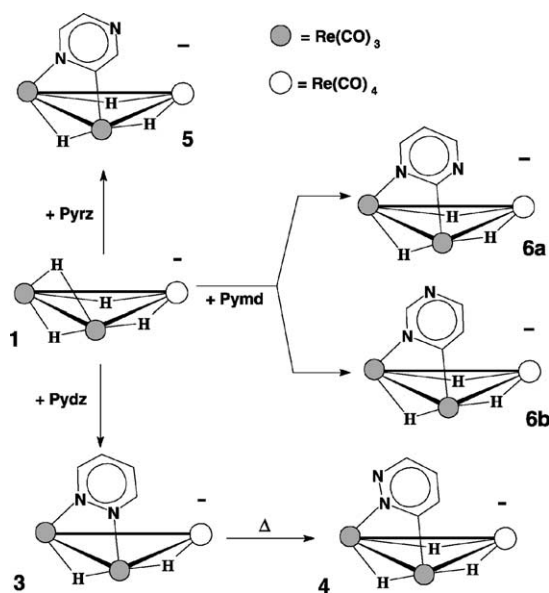
3.1. Reaction of **1** with 1,2-diazine

When the [NEt₄]⁺ salt of the unsaturated anion [Re₃(μ-H)₄(CO)₁₀]⁻ (**1**) was dissolved in pyridazine, at room temperature, the solution colour rapidly changed from bright yellow to deep green. IR monitoring showed after ca. 3 h the quantitative formation of the novel saturated cluster anion [Re₃(μ-H)₂(μ-η²-N₂C₄H₄)(CO)₁₀]⁻ (**3**, Eq. (2), Scheme 3).



The formulation of **3**, based on the spectroscopic data (IR and ¹H NMR, see Table 1), was confirmed by a single-crystal X-ray analysis (see further). The presence of two hydridic resonances indicates that one of the hydrides (H_a, responsible for the lowest field signal, on the bases of the previous empirical “additivity rules” [28–30]) is co-ordinated on the same Re–Re bond bridged by the μ-pyridazine group, as in the solid state (vide infra).

At low temperatures each of the two aromatic resonances separated into two signals, indicating the



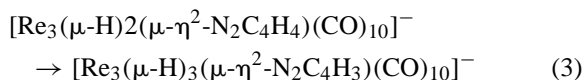
Scheme 3.

occurrence of a fluxional process (likely the hopping of the lateral hydride) that generates a mirror plane perpendicular to the plane of the cluster. This process is currently under investigation and will be described elsewhere.

The formation of **3** most likely occurs through intermediates **I1** and **I2** analogous to those proposed for the reaction of **1** with pyridine in Scheme 1: in the present case intramolecular coordination of the second nitrogen ligand in **I2** is favoured over C–H activation.

However, it was possible to obtain the orthometallated isomer of **3**, namely $[\text{Re}_3(\mu\text{-H})_3(\mu\text{-}\eta^2\text{-N}_2\text{C}_4\text{H}_3)(\text{CO})_{10}]^-$ (**4**), by using the thermal activation method described by Deeming et al. [17]. The novel species (Scheme 3, Eq. (3)) was identified by its hydridic resonances (three signals in ratio 1:1:1, at δ values very close to those exhibited by other related orthometallated derivatives, see Table 1). Moreover, the aromatic resonances are almost identical to those reported for the orthometallated 1,2-diazine moiety in

$\text{Os}_3(\mu\text{-H})(\mu\text{-}\eta^2\text{-N}_2\text{C}_4\text{H}_3)(\text{CO})_{10}$ [17].



As observed in the case of the above Os cluster [17], the thermal conversion of **3** into **4** was not a selective process and at long times extensive decomposition took place, hampering the complete conversion of **3** or the possible attainment of an equilibrium ratio.

3.2. Description of the structure of anion **3**

The crystal structure of compound $[\text{NEt}_4][\text{Re}_3(\mu\text{-H})_2(\mu\text{-}\eta^2\text{-N}_2\text{C}_4\text{H}_4)(\text{CO})_{10}]$ ($[\text{NEt}_4]\mathbf{3}$) consists of the packing of discrete cluster anions and $[\text{NEt}_4]^+$ cations in the ratio 1:1, separated by normal van der Waals contacts. The molecular structure of **3** is illustrated in Fig. 1. Anion **3** contains a triangular metal core with two longer edges [Re(1)–Re(2) and

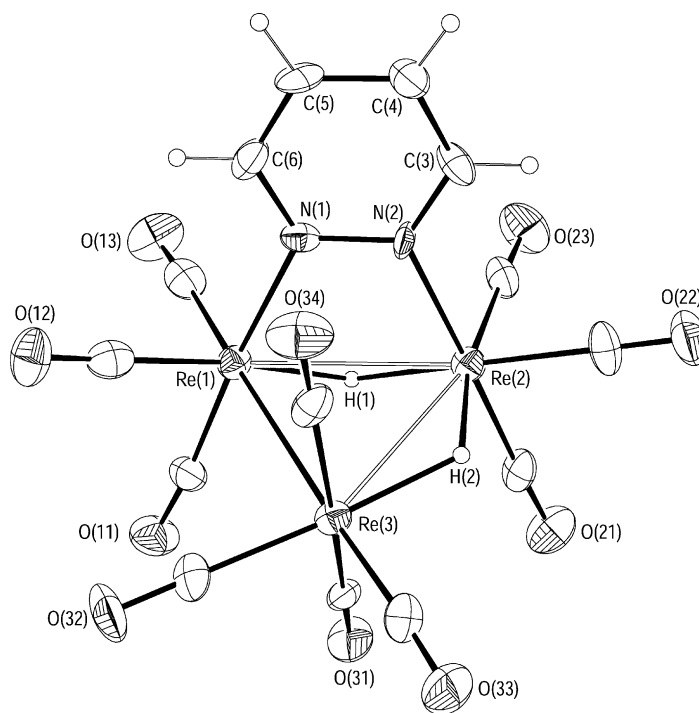


Fig. 1. ORTEP drawing of the $[\text{Re}_3(\mu\text{-H})_2(\mu\text{-}\eta^2\text{-N}_2\text{C}_4\text{H}_4)(\text{CO})_{10}]^-$ anion (**3**) with partial labeling scheme. Displacement ellipsoids are drawn at the 30% probability level. Hydrogen atoms are given arbitrary radii. Relevant bond lengths (Å): Re(1)–Re(2) 3.1153(10), Re(1)–Re(3) 2.9812(10), Re(2)–Re(3) 3.1817(10), Re(1)–N(1) 2.180(11), Re(2)–N(2) 2.162(12).

Re(2)–Re(3)], bridged by one hydrido ligand each, and one shorter edge [Re(1)–Re(3)], in correspondence with a direct metal–metal interaction. With reference to the parent cluster $[\text{Re}_3(\mu\text{-H})_2(\text{CO})_{12}]^-$ [31], two axial carbonyl ligands on two adjacent rhenium atoms are actually replaced by a bridging μ -pyridazine- $\kappa\text{N}^1:\kappa\text{N}^2$ ligand. Bond lengths for the direct Re(1)–Re(3) interaction (2.981(1) Å) and for the hydrido-bridged Re(2)–Re(3) interaction (3.182(1) Å) compares well with the values observed in the parent compound (3.035(7) and 3.177(7) Å, respectively). The bond length of the Re(1)–Re(2) edge (3.115(1) Å), which is additionally bridged by the pyridazine ligand, is similar to those found for analogous $\text{Re}(\mu\text{-H})(\mu\text{-}\eta^2\text{-X})\text{Re}$ interactions (see for example the value of 3.116(1) Å in the orthometallated pyridine derivative $[\text{Re}_3(\mu\text{-H})_3(\mu\text{-}\eta^2\text{-NC}_5\text{H}_4)(\text{CO})_{10}]^-$ **2** [19]).

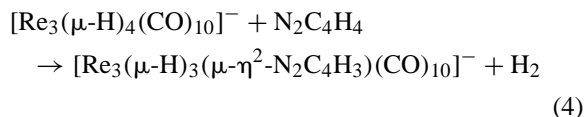
The geometry about each rhenium atom is best described as distorted octahedral, taking into account both the hydrido ligands and the direct Re(1)–Re(3) bond. All hydrido ligands were indirectly located on the basis of the stereochemistry of the other ligands and by use of potential energy calculations [27]. As expected, hydride H(1) lies opposite the μ -pyridazine ligand, 0.87 Å below the metal plane. Hydride H(2), which in the parent compound lies in the triangular plane, is here distinctly above it (0.28 Å). This can be ascribed to the steric repulsion between the axial carbonyl ligand CO(34) and the pyridazine ring, which causes a tilting of the local metal octahedra: as a result, the equatorial carbonyl ligands CO(32) and CO(33) are pushed below the Re_3 triangular plane and the Re(3)–H(2) vector, which tends to be directly trans to CO(32), is pushed above. In accord with the presence of this repulsive interaction, the pyridazine ligand shows a distinct outward folding around the Re(1)–Re(2) axis, the dihedral angle between the Re_3 plane and the pyridazine least-squares plane being 101.5(5)°.

The mean Re–N bond length in **3** (2.171(12) Å) can not be compared with other Re–pyridazine bond lengths, however it falls in the range observed for analogous complexes in which sp^2 nitrogen atoms are involved in a $\mu\text{-}\eta^2$ bridge between two rhenium atoms (see for example the values of 2.168(3), 2.178(9), and 2.18(2) Å found in $[\text{Re}_3(\mu\text{-H})_3(\mu\text{-}\eta^2\text{-pz})(\text{CO})_9(\text{Hpz})]^-$ (Hpz = pyrazole)

[32], $[\text{Re}_3(\mu\text{-H})_3\{\mu\text{-}\eta^2\text{-C(H)=N}(p\text{-Tol})\}(\text{CO})_{10}]^-$ [33], and $[\text{Re}_3(\mu\text{-H})_3(\mu\text{-}\eta^2\text{-NC}_5\text{H}_4)(\text{CO})_{10}]^-$ [19], respectively). The pyridazine ring is perfectly planar, the maximum deviation from the least-squares plane being 0.012(12) Å. The carbonyl ligands are linear, with Re–C–O angles between 174.4(16) and 179.5(16)°.

3.3. Reaction of **1** with 1,4-diazine

The reaction was performed at 60 °C in molten pyrazine (mp 53 °C). After ca. 1.5 h spectroscopic analyses revealed the selective formation of the novel saturated anion **5**, containing an orthometallated pyrazine (Eq. (4), Scheme 3), characterised by ^1H NMR (see Table 1).



In contrast to the case of pyridine [20], the oxidative addition of pyrazine was substantially irreversible, the amount of **1** not exceeding 5% after 7 days under 100 atm of H_2 .

3.4. Reaction of **1** with 1,3-diazine

Upon stirring the anion **1** in freshly distilled pyrimidine at room temperature for a few days, we obtained roughly equimolar amounts of two isomeric forms of the orthometallated derivative **6** (Scheme 3), arising from the activation of the two different *ortho* positions of pyrimidine (C2 and C6, see Scheme 2). The reaction followed a clean first order path up to more than three half-life periods (Fig. 2), with a rate about one order of magnitude smaller than in the case of pyridine ($2.0 \times 10^{-5} \text{ s}^{-1}$ versus $2.1 \times 10^{-4} \text{ s}^{-1}$). The two isomers have been clearly distinguished on the basis of their different coupling pattern in the aromatic region of the ^1H NMR spectra (Table 1).

^1H NMR monitoring, in non-deuterated pyrimidine solution (Fig. 2), showed that at longer times the isomer **6b** was slightly dominant (ratio 1.24 at complete conversion). This might be the result of a small kinetic preference for **6b**, possibly attributable to a lower donor power of the C2–H bond (in *ortho* to

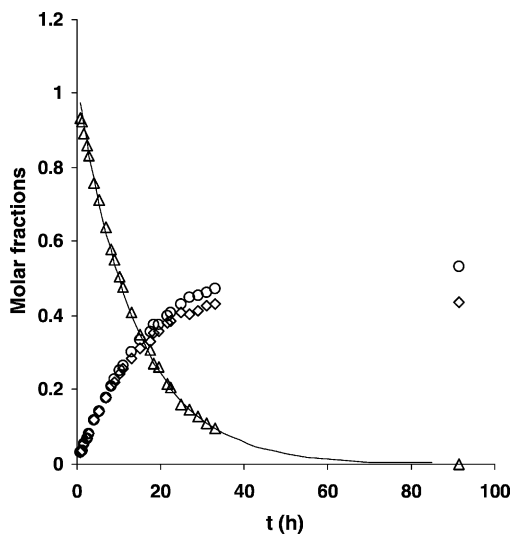


Fig. 2. Time course of the reaction of **1** in pyrimidine solution at 300K: **1** (Δ), **6a** (\diamond) and **6b** (\circ). The line represents the concentrations of **1** calculated on using the first-order kinetic constant ($k_{\text{obs}} = 2.0 \times 10^{-5} \text{ s}^{-1}$) obtained from the least-squares fit of the experimental data.

two N atoms) with respect to the C6–H bond, in the agostic interaction preceding the oxidative addition. Alternatively, the rate of formation of the two isomers might be substantially identical, and a successive slow conversion of **6a** into **6b** should account for the trend observed at longer times. It was impossible to establish with certainty if this **6a** \rightarrow **6b** conversion does occur (and to estimate a possible equilibrium ratio), since in a separate experiment we observed that pyrimidine solutions containing mixtures of **6a** and **6b** slowly gave rise to the formation of two novel species **7a** and **7b** (Fig. 3). These compounds have been tentatively formulated as two isomers of the $[\text{Re}_3(\mu\text{-H})_3(\mu\text{-}\eta^2\text{-N}_2\text{C}_4\text{H}_3)(\text{pymd})(\text{CO})_9]^-$ anion (see Scheme 4), on the bases of their hydridic δ values (see Table 1), quite similar to those of the previously known derivative $[\text{Re}_3(\mu\text{-H})_3(\mu\text{-}\eta^2\text{-NC}_5\text{H}_4)(\text{py})(\text{CO})_9]^-$, containing a pyridine terminally coordinated on the vertex of the cluster [19]. The two isomers **7a** and **7b** have been obtained in higher amounts by heating **1** in pyrimidine at 85 °C for 2 h, thus allowing their complete NMR characterisation. The splitting pattern of the aromatic protons, similar to those of **6a** and **6b** respectively

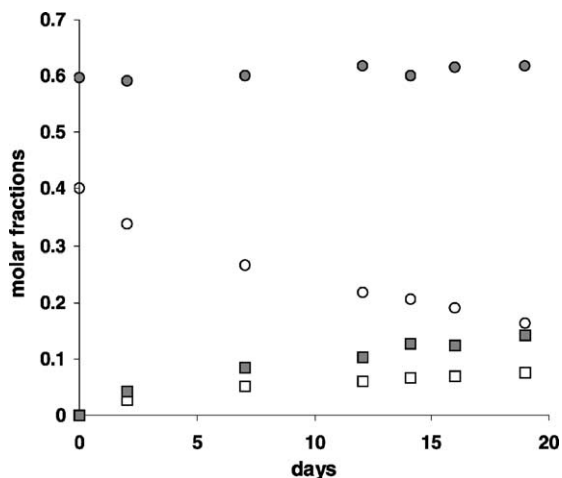
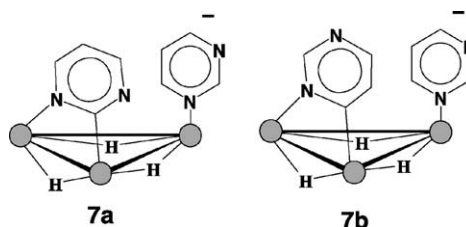


Fig. 3. Time course of the concentrations of **6a** (\circ), **6b** (\bullet), **7a** (\square) and **7b** (\blacksquare), starting from a 2:3 mixture of **6a** and **6b**, in pyrimidine solution at room temperature.

(see Table 1), suggests the formulations shown in Scheme 4.

The data of Fig. 3 (pyrimidine solution) seem to indicate that the formation of **7** occurred at the expenses of the only isomer **6a**. However, the formulations of **7a** and **7b** shown in Scheme 4 support the idea that they arose from **6a** and **6b**, respectively. This hypothesis implies a slow **6a** \rightarrow **6b** transformation preceding the formation of **7b**, to account for the constancy of the amount of **6b**.

In CD_2Cl_2 no evidence of **6a** \rightarrow **6b** conversion was obtained, after 7 days at room temperature, in a reaction mixture analogous to that of Fig. 3. Moreover, in the same solvent under 100 atm of H_2 we observed the formation of only a small amount of **1** (ca. 15% after 5 days), at the expenses of both **6a** and **6b**.



Scheme 4.

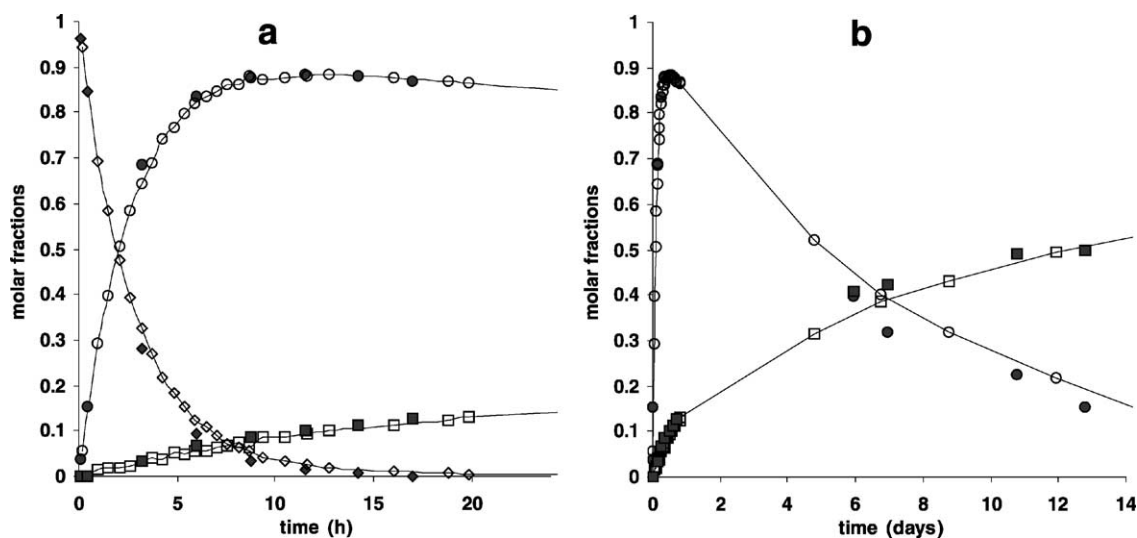


Fig. 4. Time course of the two competition reactions performed on dissolving **1** in equimolar mixtures of (i) pyridine and pyrazine (open symbols linked by a line) or (ii) pyridine and pyrimidine (filled symbols, without connecting line): **1** (\diamond and \blacklozenge), **2** (\circ and \bullet), **5** (\square) and **6** (\blacksquare , **6a** + **6b**). Plot (a) refers to the initial times and (b) depicts the overall reaction course.

3.5. Competition for C–H activation between pyridine, pyrazine and pyrimidine

A sample of $[\text{NEt}_4]\mathbf{1}$ was dissolved in an equimolar mixture of pyridine and pyrazine and the progress of the reaction was monitored by ^1H NMR at room temperature. The spectra showed the fast disappearance of **1** to give mainly the orthometallated pyridine derivative **2** (\circ , open circle, in Fig. 4), accompanied by a much smaller amount of **5** (\square , open square in the Fig. 4), arising from activation of the C–H bond of pyrazine (ratio **5/2** about 0.04 at ca. 50% of conversion of **1**). The concentration of **2** attained a maximum after ca. 10 h, when the reactant **1** was almost completely disappeared and then slowly decreased, to give **5** (Fig. 4b). The same reaction course was observed in a similar competition experiment between pyridine and pyrimidine (shown in Fig. 4 with analogous, but filled symbols): initially **1** afforded mainly **2**, with a rate similar to that observed in the previous experiment, and at longer times **2** slowly converted into **6a** and **6b**, arising from pyrimidine activation. In both cases, several minor unidentified hydridic by-products were formed (their overall final amount corresponding to ca. 30% of the overall integrated hydridic intensity).

4. Conclusions

Different types of competition have been tested in this work. The preferred formation of **3** rather than **4** in the reaction of **1** with 1,2-diazine shows that in the intermediate analogous to **I2** of Scheme 1 the *intramolecular* coordination of the second pyridinic nitrogen is favoured over *ortho* C–H activation. This is likely attributable to a lower activation barrier, nitrogen coordination requiring much smaller rearrangements than orthometallation. This is confirmed by the **3** \rightarrow **4** conversion observed at higher temperatures.

In the same key intermediate **I2** the *intramolecular* *ortho* C–H activation is favoured with respect to the *intermolecular* coordination of a second nitrogen atom. Indeed, in no cases did we observe disubstituted $[\text{Re}_3(\mu\text{-H})_2(\text{CO})_{10}(\text{azine})_2]^-$ derivatives: such species are probably present when the azine itself is the solvent, as weakly stabilised forms of **I2**, but the second azine is easily displaced by C–H addition.

In the case of 1,3-diazine a slight preference for the activation of the C6–H bond has been observed, as reported also in the two previous cases in which pyrimidine orthometallation was described, i.e. in the clusters $[\text{M}_3(\mu\text{-H})(\mu\text{-}\eta^2\text{-N}_2\text{C}_5\text{H}_3)(\text{CO})_{10}]$ ($\text{M} = \text{Ru}$ [18] or Os [17]).

The formation of the orthometallated derivatives of 1,3 and 1,4 diazines was much slower than in the case of pyridine, as shown by the comparison of the kinetic constants for the disappearance of **1** (see further) and by the competition experiments of Fig. 4. This is likely due the slower formation of intermediate **II**, due to the lower basicity of diazines with respect to pyridine (pK_a 0.65 for pyrazine and 1.23 for pyrimidine versus 5.23 for pyridine).

A second major difference in the behaviour of these diazines with respect to pyridine concerns the reversibility of the oxidative addition, that in pyridine is much easier than in 1,3 or 1,4 diazines. This difference can be attributed to the fact that the *ortho* positions of pyrazine and pyrimidine are more electron-deficient than the *ortho* position of pyridine, due to the presence of the second nitrogen atom. The interesting consequence of these points is that the competition between pyridine and diazines affords the anion **2** (containing orthometallated pyridine) as the kinetic product, and anions **5** or **6** (containing orthometallated diazines) as the thermodynamically favoured products (due to the irreversibility of their formation).

Acknowledgements

We thank Italian MIUR (Project Metal Clusters: Basic and Functional Aspects) for financial support and CNR-ISTM for providing instrumental facilities.

References

- [1] R.H. Fish, in: R. Ugo (Ed.), Aspect of Homogeneous Catalysis, vol. 7, Kluwer Academic Publishers, The Netherlands, 1990, p. 65.
- [2] R.J. Angelici, Polyhedron 16 (1997) 3088.
- [3] K.J. Weller, P.A. Fox, S.D. Gray, D.E. Wigley, Polyhedron 16 (1997) 3139.
- [4] E.C. Constable, Polyhedron 3 (1984) 1037.
- [5] D.F. Shriver, H.D. Kaesz, R.D. Adams, The Chemistry of Metal Clusters Complexes, VCH, Weinheim, 1990.
- [6] P. Braunstein, L.A. Oro, P.R. Raithby, Metal Clusters in Chemistry, VCH, Weinheim, 1999.
- [7] R.D. Adams, F.A. Cotton, Catalysis by Di- and Polynuclear Metal Cluster Complexes, Wiley, New York, 1998.
- [8] R.D. Adams, I.T. Horváth, Progr. Inorg. Chem. 33 (1985) 127.
- [9] H. Suzuki, Eur. J. Inorg. Chem. (2002) 1009.
- [10] R.B. Calvert, J.R. Shapley, J. Am. Chem. Soc. 99 (1977) 5225.
- [11] P.M. Duggan, D.J. Barnett, M.J. Muscatella, J.B. Keister, J. Am. Chem. Soc. 108 (1986) 6076.
- [12] T.K. Dutta, J.C. Vites, G.B. Jacobsen, T.P. Fehlner, Organometallics 6 (1987) 842.
- [13] E. Rosenberg, Md.J. Abedin, D. Rokhsana, D. Osella, L. Milone, C. Nervi, J. Fiedler, Inorg. Chim. Acta 300 (2000) 769.
- [14] Md.J. Abedin, B. Bergman, R. Holmquist, R. Smith, E. Rosenberg, J. Ciurash, K. Hardcastle, J. Roe, V. Vazquez, C. Roe, S. Kabir, B. Roy, S. Alam, K.A. Azam, Coord. Chem. Rev. 190 (1999) 975.
- [15] E. Arcia, D.S. Kolwaite, E. Rosenberg, K. Hardcastle, J. Ciurash, R. Duque, R. Gobetto, L. Milone, D. Osella, M. Botta, W. Dastrù, A. Viale, I. Fiedler, Organometallics 17 (1998) 415.
- [16] R. Agarwala, K.A. Azam, R. Dilshad, S.E. Kebir, R. Miah, M. Shahiduzzaman, K.I. Hardcastle, E. Rosenberg, M.B. Hursthouse, K.M.A. Malik, J. Organomet. Chem. 492 (1995) 135.
- [17] A.J. Deeming, R. Peters, M.B. Hursthouse, J.D.J. Backer-Dirks, J. Chem. Soc., Dalton Trans. (1982) 787.
- [18] G.A. Foulds, B.F.G. Johnson, J. Lewis, J. Organomet. Chem. 294 (1985) 123.
- [19] T. Beringhelli, G. D'Alfonso, G. Ciani, D.M. Proserpio, A. Sironi, Organometallics 12 (1993) 4863.
- [20] T. Beringhelli, L. Carlucci, G. D'Alfonso, G. Ciani, D.M. Proserpio, J. Organomet. Chem. 504 (1995) 15.
- [21] D.F. Shriver, M.A. Drezdson, The Manipulation of Air Sensitive Compounds, second ed., Wiley/Interscience, New York, 1986.
- [22] H.C. Horng, C.P. Cheng, C.S. Yang, G.H. Lee, Organometallics 15 (1996) 2543.
- [23] T. Beringhelli, G. D'Alfonso, M.G. Garavaglia, J. Chem. Soc., Dalton. Trans. (1996) 1771.
- [24] A.C.T. North, D.C. Phillips, F.S. Mathews, Acta Crystallogr., Sect. A 24 (1968) 351.
- [25] A. Altomare, M.C. Burla, M. Camalli, G.L. Cascarano, C. Giacovazzo, A. Guagliardi, A.G.G. Moliterni, G. Polidori, R. Spagna, J. Appl. Crystallogr. 32 (1999) 115.
- [26] G.M. Sheldrick, SHELX97, Universität Göttingen, Germany, 1997.
- [27] A.G. Orpen, J. Chem. Soc., Dalton Trans. (1980) 2509.
- [28] T. Beringhelli, G. D'Alfonso, M. Freni, G. Ciani, M. Moret, A. Sironi, J. Chem. Soc., Dalton Trans. (1989) 1143.
- [29] T. Beringhelli, G. D'Alfonso, M. Freni, G. Ciani, A. Sironi, H. Molinari, J. Chem. Soc., Dalton Trans. (1986) 2691.
- [30] T. Beringhelli, G. D'Alfonso, M. Panigati, J. Organomet. Chem. 527 (1997) 215.
- [31] M.R. Churchill, P.H. Bird, H.D. Kaesz, R. Bau, B. Fontal, J. Am. Chem. Soc. 90 (1968) 7135.
- [32] T. Beringhelli, G. D'Alfonso, M. Panigati, F. Porta, P. Mercandelli, M. Moret, A. Sironi, Organometallics 17 (1998) 3282.
- [33] T. Beringhelli, G. D'Alfonso, A. Minoja, G. Ciani, M. Moret, A. Sironi, Organometallics 10 (1991) 3131.